Callose Synthase GSL7 Is Necessary for Normal Phloem Transport and Inflorescence Growth in Arabidopsis[1][W][OA]

D.H. Paul Barratt, Katharina Kölling, Alexander Graf[2], Marilyn Pike, Grant Calder, Kim Findlay, Samuel C. Zeeman, and Alison M. Smith*

John Innes Centre, Norwich Research Park, Colney, Norwich NR4 7UH, United Kingdom (D.H.P.B., A.G., M.P., G.C., K.F., A.M.S.); and Department of Biology, Eidgenössisch Technische Hochschule Zurich, CH–8092 Zurich, Switzerland (K.K., S.C.Z.)

One isoform of callose synthase, Glucan Synthase-Like7 (GSL7), is tightly coexpressed with two isoforms of sucrose synthase (SUS5 and SUS6) known to be confined to phloem sieve elements in Arabidopsis (*Arabidopsis thaliana*). Investigation of the phenotype of *gsl7* mutants of Arabidopsis revealed that the sieve plate pores of stems and roots lack the callose lining seen in wild-type plants. Callose synthesis in other tissues of the plant appears to be unaffected. Although *gsl7* plants show only minor phenotypic alterations during vegetative growth, flowering stems are reduced in height and all floral parts are smaller than those of wild-type plants. Several lines of evidence suggest that the reduced growth of the inflorescence is a result of carbohydrate starvation. Levels of sucrose, hexoses, and starch are lower in the terminal bud clusters of *gsl7* than in those of wild-type plants. Transcript levels of "starvation" genes expressed in response to low sugars are elevated in the terminal bud clusters of *gsl7* plants, at the end of the night, and during an extended night. Pulse-chase experiments with $^{14}CO_2$ show that transport of assimilate in the flowering stem is much slower in *gsl7* mutants than in wild-type plants. We suggest that the callose lining of sieve plate pores is essential for normal phloem transport because it confers favorable flow characteristics on the pores.

The pores in the sieve plates of phloem elements are key determinants of the velocity of transport of Suc and other phloem contents over long distances in the plant. From theoretical models, phloem conductance is predicted to be directly related to the density of pores on the sieve plate and to the length and diameter of the pores (Thompson and Holbrook, 2003; Thompson, 2006). During phloem development, pore formation is preceded by deposition of the β1,3-glucan callose between the plasma membrane and the cell wall, both as "platelets" on the faces of the end wall and around the plasmodesmatal channel. The pore is formed by widening of the plasmodesmatal channel, a process that involves removal of some of the callose. The precise sequence of events, and the importance of callose in these events, remain unclear. Some authors propose that callose largely replaces cellulose in the region of the wall in which the sieve plate pore will form. Pore formation is then due primarily to callose degradation (Esau and Thorsch, 1985; Thorsch and Esau, 1988). Others reject the idea that callose replaces original cell wall material and propose that pore formation involves degradation of the original material as well as some callose. According to this view, the main function of callose deposition is to restrict wall thickening in the region in which the pore will form (Evert et al., 1966; Deshpande, 1974, 1975).

However it is derived, the mature pore usually has a callose lining (Bouck and Cronshaw, 1965; Deshpande, 1974, 1975; Thorsch and Esau 1988; Eleftheriou, 1990; for summary, see Sjölund, 1997). If mature phloem elements are damaged, massive callose synthesis occurs on the sieve plate, resulting in occlusion of the pores and retention of phloem contents behind the callose plugs (Evert and Derr, 1964; Hao et al., 2008; Mullendore et al., 2010). Indeed, because callose is formed very rapidly upon damage to the phloem, its existence in sieve plate pores in undamaged plants has been disputed in the past: some authors have argued that its presence is an artifact of sectioning and preparation techniques (Evert and Derr, 1964; Walsh and Melaragno, 1976; Spanner, 1978; Sjölund, 1997; for summary, see van Bel, 2003). However, callose linings have been observed in sieve plate pores from a wide

[1] This work was supported by a core strategic grant awarded by the Biotechnology and Biological Sciences Research Council (UK) to the John Innes Centre, by the John Innes Foundation (research studentship to A.G.), by the Swiss National Science Foundation (via the SystemsX.ch initiative Plant Growth in a Changing Environment), and by Eidgenössisch Technische Hochschule Zurich.

[2] Present address: Department of Biology, Eidgenössisch Technische Hochschule Zurich, Universitätsstrasse 2, CH–8092 Zurich, Switzerland.

* Corresponding author; e-mail alison.smith@bbsrc.ac.uk.

The author responsible for distribution of materials integral to the findings presented in this article in accordance with the policy described in the Instructions for Authors (www.plantphysiol.org) is: Alison M. Smith (alison.smith@bbsrc.ac.uk).

[W] The online version of this article contains Web-only data.

[OA] Open Access articles can be viewed online without a subscription.

www.plantphysiol.org/cgi/doi/10.1104/pp.110.166330

range of plant species and organs and with a range of techniques designed to minimize the possibility of callose synthesis during tissue preparation (Ehlers et al., 2000; van Bel et al., 2002). They are almost certainly a feature of mature sieve plates in many species.

Callose synthesis occurs during normal growth in many locations in plants. In addition to sieve plate pores, it is deposited in the cell plate during cytokinesis (Samuels et al., 1995), in cell walls at the neck region of plasmodesmata (Turner et al., 1994), and during pollen formation (microgametogenesis) and pollen tube growth (Rae et al., 1985; McCormick, 1993). It is also deposited on the inner face of cell walls in response to pathogen attack, forming a barrier against fungal penetration (Jacobs et al., 2003; Nishimura et al., 2003). Callose is synthesized from the sugar nucleotide UDPglucose via callose synthases that span the plasma membrane. In both vascular and nonvascular plants, callose synthases are encoded by multigene families, and different isoforms have different locations and functions in the plant (Voigt et al., 2006; Dong et al., 2008; Schober et al., 2009; Schuette et al., 2009). Of the 12 *Glucan Synthase-Like* (*GSL*; also called *CalS*) genes in Arabidopsis (*Arabidopsis thaliana*), five are suggested or proven from mutational and correlative analyses to encode isoforms with important functions in pollen development (*GSL1*, *GSL2*, *GSL5*, *GSL8*, and *GSL10*; Enns et al., 2005; Nishikawa et al., 2005; Töller et al., 2008; Huang et al., 2009). Two genes have been implicated in cytokinesis, cell plate formation, and cell patterning (*GSL6* and *GSL8*; Hong et al., 2001; Chen et al., 2009; Thiele et al., 2009) and one in response to attack by fungal pathogens (*GSL5*; Jacobs et al., 2003; Nishimura et al., 2003; Dong et al., 2008). Expression of the *GSL6* gene is elevated and callose is deposited locally in response to phloem feeding by silverleaf whitefly nymphs (*Bemisia* sp.; Kempema et al., 2007) and the aphid *Brevicoryne brassicae* (Kuśnierczyk et al., 2008). The isoform(s) responsible for the synthesis of callose in sieve plate pores has yet to be identified.

Interest in the control of phloem transport has increased with the demonstration of its importance in the transmission of developmental and environmentally triggered signaling molecules involved in the induction of flowering and of systemic resistance to pathogens (Turgeon and Wolf, 2009). There has been recent progress in modeling phloem transport and in the precise measurement of anatomical features and transport velocity (Van As, 2007; Mullendore et al., 2010). These approaches reveal that callose deposition in sieve plate pores after wounding can drastically reduce phloem conductivity within minutes. They also suggest that there is a much more complex relationship between phloem conductivity (estimated from anatomical measurements) and the velocity of phloem transport (measured by MRI) across species than is predicted from simple microfluidic principles. Further progress in this area is likely to be slow without new tools to manipulate anatomical components of the phloem in a precise, specific, and noninvasive manner within a single species.

We discovered recently that the synthesis of the callose lining of pores in the phloem sieve plates of the flowering stem of Arabidopsis is partially dependent upon the presence of two isoforms of Suc synthase, SUS5 and SUS6. In a mutant lacking both isoforms (the *sus5sus6* mutant), the thickness of the callose lining is markedly reduced but callose formation is normal in other parts of the plant (Barratt et al., 2009). SUS5 and SUS6 appear to be present exclusively in the phloem. In roots, both transcripts are reported to be phloem located (Birnbaum et al., 2003; http://www.arexdb.org/root-images/deconRoot.html), and in situ hybridizations detected SUS6 transcript only in phloem initial cells (Barratt et al., 2009). Immunoblots of tissue prints revealed SUS5 and SUS6 proteins only in phloem tissue in stems and mature hypocotyls. Taken together, these data indicate that SUS5 and SUS6 may have a specific role in the provision of the UDPglucose substrate for the synthesis of callose in the wall of sieve plate pores.

To discover further components of the pathway of callose synthesis in the sieve plate, and thus provide tools for exploring the role of this polymer in the development and function of the phloem, we looked for genes that are coexpressed with *SUS5* and/or *SUS6*. We found that *SUS5*, *SUS6*, and one callose synthase, *GSL7*, are tightly coexpressed. Here, we show that *GSL7* is expressed in the phloem and is necessary for callose synthesis in the sieve plate. In *gsl7* mutants, growth of the floral stem and all floral parts is reduced. We provide evidence that this is due to carbon starvation caused by reduced phloem conductivity.

RESULTS

Identification of *GSL7* as a Gene Coexpressed with *SUS5* and *SUS6*

Two different coexpression databases (ATTED-II, the Arabidopsis trans-factor and cis-element prediction database [Obayashi et al., 2007], http://atted.jp/; AthCoR@CSB.DB, the Arabidopsis coresponse database, http://csbdb.mpimp-golm.mpg.de/csbdb/dbcor/ath/ath_tsgq.html, "developmental series") revealed a strong correlation between the abundance of transcripts for *SUS5*, *SUS6*, and a gene encoding a putative callose synthase, *GSL7* (*CalS7*; At1g06490). This correlation is particularly striking because it was identified in both databases. The lists of genes coexpressed with *SUS5* otherwise showed very little similarity between the two databases (Supplemental Tables S1 and S2).

In whole-mount in situ hybridization experiments on roots, *GSL7* transcript was detected only in two discrete regions in the differentiating stele. No tran-

script was detected using a sense probe as a control (Fig. 1). This distribution is very similar to that of *SUS6* transcript (Barratt et al., 2009) and is consistent with the idea that *GSL7* transcript may be located in the phloem initial cells. Further evidence of a phloem location is provided by global analyses of patterns of gene expression in the Arabidopsis root (Birnbaum et al., 2003; Brady et al., 2007; Cartwright et al., 2009; Arex, the Arabidopsis Gene Expression database, http://www.arexdb.org/). Transcript levels for *SUS5*, *SUS6*, and *GSL7* are strongly enhanced in the phloem relative to all other cell types in the root (Supplemental Fig. S1).

Loss of GSL7 Eliminates Callose from Phloem Sieve Plates

To discover the role and importance of GSL7, we obtained insertion mutants from the SALK and Syngenta Arabidopsis Insertion Library (SAIL) collections. Homozygous lines were named *gsl7-1* (SALK_048921) and *gsl7-2* (SAIL_114_A01). *GSL7* transcript was not detectable in stems of either of these lines (Supplemental Fig. S2).

To visualize callose, sections of flowering stem were stained with aniline blue, a dye that fluoresces when it binds callose. Callose was present in the phloem region in hand-cut sections of stems of wild-type plants but not *gsl7* mutant plants (Fig. 2A, arrows). Prolonged (18-h) incubation of cut stems in water prior to fixation and sectioning failed to induce callose formation in the phloem in mutant plants (Fig. 2B).

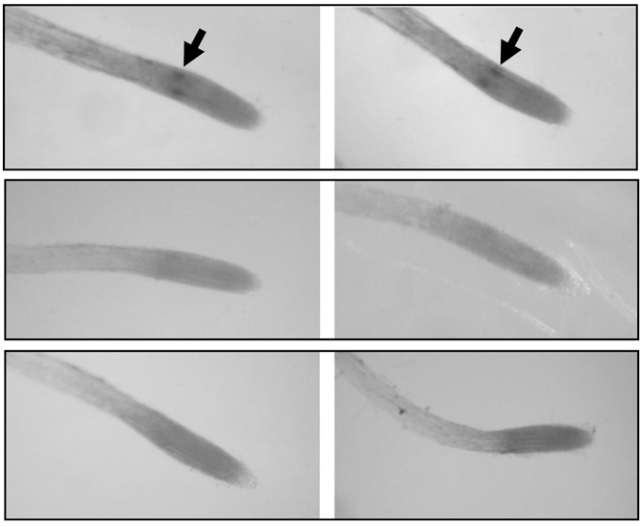

Figure 1. Location of transcription of the *GSL7* gene in roots. Whole-mount preparations of roots were treated with antisense and sense probes from the *GSL7* gene. A, Two examples of roots from wild-type plants probed with a 350-bp antisense probe. The arrows indicate two regions of hybridization within the root. B, Two examples of wild-type roots probed with a 350-bp sense probe. C, Two examples of roots from *gsl7* mutant plants probed with a 350-bp antisense probe.

However, callose formation was induced in cells adjacent to the xylem in both wild-type and mutant plants (Fig. 2B, stars).

Aniline blue staining of whole roots also indicated a specific role for GSL7 in callose production in the phloem. In wild-type roots, callose was abundant in single files of cells in the stele of older parts of the root. No callose was visible in this location in *gsl7* mutant roots (Fig. 3).

These observations suggested that GSL7 is responsible for the production of callose in the phloem but not for the production of callose in other cell types, either when intact or in response to wounding. To test this idea further, we examined callose production in response to mechanical wounding of mature leaves. The deposition of callose around mesophyll cells bordering the wound site was indistinguishable in wild-type and *gsl7* plants (Fig. 2C).

To discover the location of GSL7-dependent callose in the phloem and to establish whether GSL7 is responsible for callose in the phloem of intact as well as wounded plants, we examined transmission electron micrographs of longitudinal sections of flowering stems and older regions of seedling roots. To prevent the production of wound callose, tissues were excised into fixative and immediately vacuum infiltrated. In wild-type plants, sieve plate pores in both flowering stems and roots were lined with callose (Figs. 2 and 3; Barratt et al., 2009). By contrast, no callose lining was visible in sieve plate pores in either stems or roots of the *gsl7* mutant. Immunogold labeling with a callose-specific antiserum confirmed the presence of callose in the lining of the sieve plate pores in the wild type but failed to detect callose in the pore walls of the mutant (Fig. 2; data not shown).

To obtain more information about the impact of the loss of GSL7 on sieve plate anatomy, we used high-resolution confocal laser scanning microscopy on thick sections of flowering stems after rapid fixation and pseudo-Schiff propidium iodide staining. As reported previously (Truernit et al., 2008), this allowed transverse and longitudinal resolution of sieve plates (Fig. 4). In wild-type plants, sieve plate pores were large and unobstructed (Fig. 4A). Measurements of 20 sieve plates (from at least two stems in each of two separate preparations) gave pore diameters between 0.30 and 0.55 μm. These data accord well with previous estimates for Arabidopsis stems of approximately 0.5 μm (1-week-old stems; Truernit et al., 2008) and 0.52 μm (stems of unspecified age; Thompson and Wolniak, 2008). By contrast, although pore numbers per sieve plate were approximately the same as in wild-type plants, sieve plate pores in stems of mutant plants appeared much smaller in diameter than those in wild-type plants. In two out of three independent preparations, pores were barely visible (Fig. 4B). In the third preparation, pores were of greater diameter (Fig. 5). Pore diameter was 0.22 $\pm$ 0.01 μm (mean $\pm$ SE of measurements on 13 sieve plates), whereas in equivalent tissue from wild-type plants grown at the same

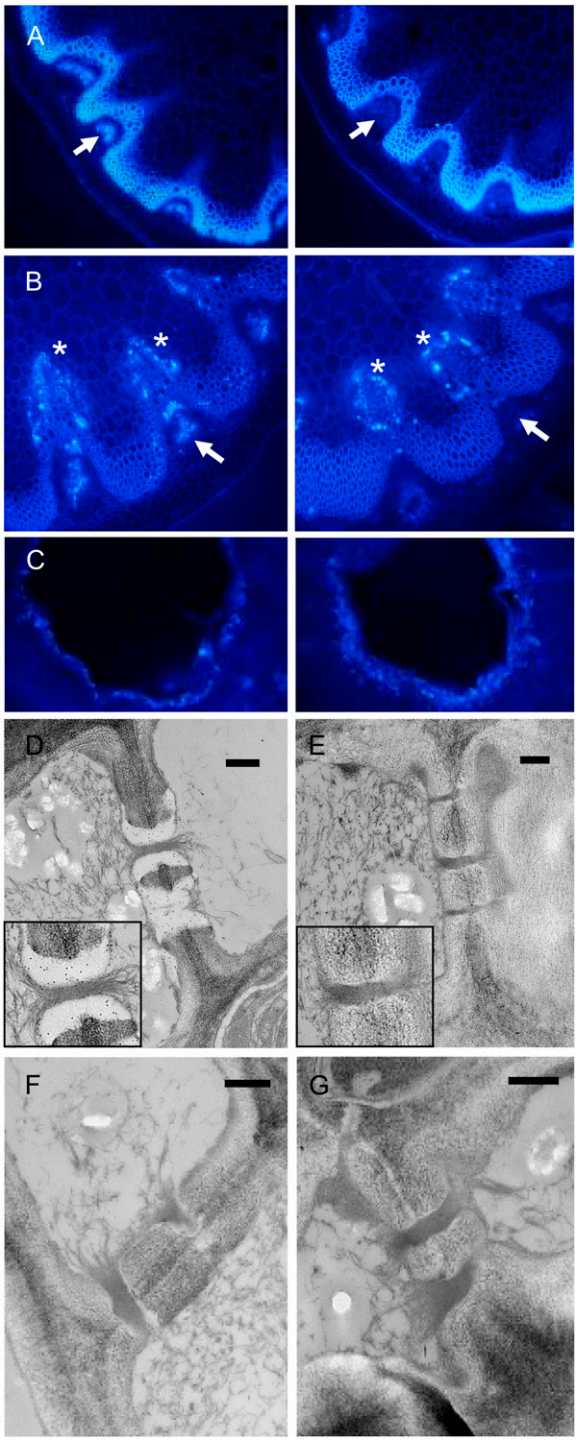

Figure 2. Loss of callose from the phloem in flowering stems of the *gsl7* mutant. All images are representative of results obtained from several different wild-type and *gsl7* mutant plants. The cell walls of the xylem and fibers are autofluorescent. A, The basal 1 to 2 cm of flowering stems from 45-d-old plants was excised, and hand-cut sections were stained with aniline blue and viewed with a UV epifluorescence microscope. Left, wild-type plant; right, *gsl7* mutant plant. Arrows indicate the position of the phloem. Fluorescence indicating the presence of callose is associated with the phloem in the wild type but not in the *gsl7* mutant. B, As in A, but excised stems were incubated in water for 18 h prior to staining. Left, wild-type plant; right, *gsl7* mutant plant. Fluorescence indicating the presence of callose is associated with cells adjacent to the xylem in both wild-type and *gsl7* mutant stems (asterisks) but is associated with the phloem only in wild-type stems (arrows). C, Fully expanded leaves from 42-d-old plants were punctured with a plastic tip and then harvested the next day, stained with aniline blue, and viewed with a UV epifluorescence microscope. Left, wild-type plant; right, *gsl7* mutant plant. D to G, Electron micrographs of phloem elements in sections of the basal 1 to 2 cm of flowering stems from wild-type (D) and *gsl7* mutant (E–G) 45-d-old plants excised directly into glutaraldehyde fixative. Sections in D and E are immunogold labeled with an anti-callose antiserum. Note the presence of gold particles in the electron-transparent sieve plate lining of wild-type plants and their absence from an equivalent position in mutant plants (compare enlarged insets in D and E). Bars = 500 nm.

time it was 0.35 ± 0.01 μm (mean ± SE of measurements on 10 sieve plates). The sieve plates themselves were similar in diameter in mutant and wild-type plants. In the preparation shown in Figure 5, sieve plate diameter was 5.40 ± 0.12 μm (10 sieve plates) in wild-type plants and 5.19 ± 0.20 μm (13 sieve plates) in mutant plants. This is comparable with previous estimates for Arabidopsis stems of between 5 and 6.2 μm (Truernit et al., 2008).

Stems and Floral Parts Are Reduced in Size in the *gsl7* Mutant

The *gsl7* mutants displayed distinct but mild phenotypes during vegetative growth (Supplemental Fig. S3). The growth rate and general morphology of *gsl7* and wild-type rosettes were very similar, as were the root and aboveground biomass at the point of emergence of the flowering stem (Fig. 6A; Supplemental Table S3). The degree of purple pigmentation of *gsl7* rosettes was greater than in wild-type plants of the same age, particularly in older rosettes (Supplemental Fig. S3).

Marked differences between *gsl7* and wild-type plants became apparent as soon as the flowering stem started to elongate. The stem was thinner in *gsl7* than in wild-type plants (Supplemental Table S3), its growth rate was slower, and the main stem and side branches of *gsl7* plants typically achieved only about half the height of those of wild-type plants. Side branches were longer in relation to the main stem in *gsl7* than in wild-type plants (Fig. 6B; Supplemental Fig. S3). The number and size of flowers and the length of peduncles and siliques were also reduced in *gsl7* mutants. Whereas sepals were of near-normal size, the lengths of petals, stamens, and carpels were reduced by one-third to one-half in mutant relative to wild-type plants (Fig. 6, C–E).

Phloem Transport Rates and Carbohydrate Availability Are Reduced in the Inflorescences of the *gsl7* Mutant

We reasoned that the reduced size of stems and floral parts in the *gsl7* mutants could be due to a limited

supply of Suc from the leaves brought about by malfunction of phloem sieve elements in the stem.

To investigate the efficiency of the transport of Suc through the flowering stem, single leaves of intact plants with 15-cm-high flowering stems were exposed to $^{14}CO_2$ in the light for 5 min. Progression of assimilated ^{14}C up the main flowering stem was measured at intervals during a 240-min chase period in the light in air (Fig. 7). Although different individual plants incorporated different amounts of ^{14}C, there was no difference between wild-type and mutant plants and the pattern of distribution of ^{14}C in the plant was not related to the total amount incorporated. Over the first 120 min of the chase period, the percentage of total

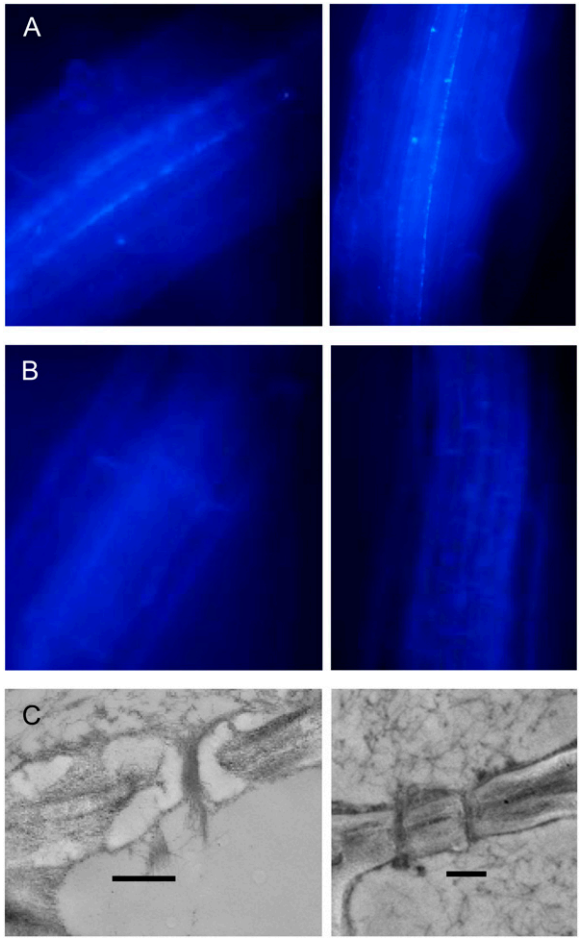

Figure 3. Loss of callose from the phloem in roots of the *gsl7* mutant. All images are representative of results obtained from several different wild-type and *gsl7* mutant plants. Photographs are of roots from 4-d-old seedlings. A and B, Regions behind the expansion zones of roots from two different seedlings stained with aniline blue. In wild-type seedlings (A), fluorescence is associated with two cell files in the stele. In *gsl7* seedlings (B), no fluorescence is visible in these cell files. C, Electron micrographs of phloem elements in sections of the proximal region of roots of wild-type (left) and *gsl7* mutant (right) seedlings. An electron-transparent lining is present in the sieve plate pores of wild-type but not *gsl7* plants. Bars = 500 nm.

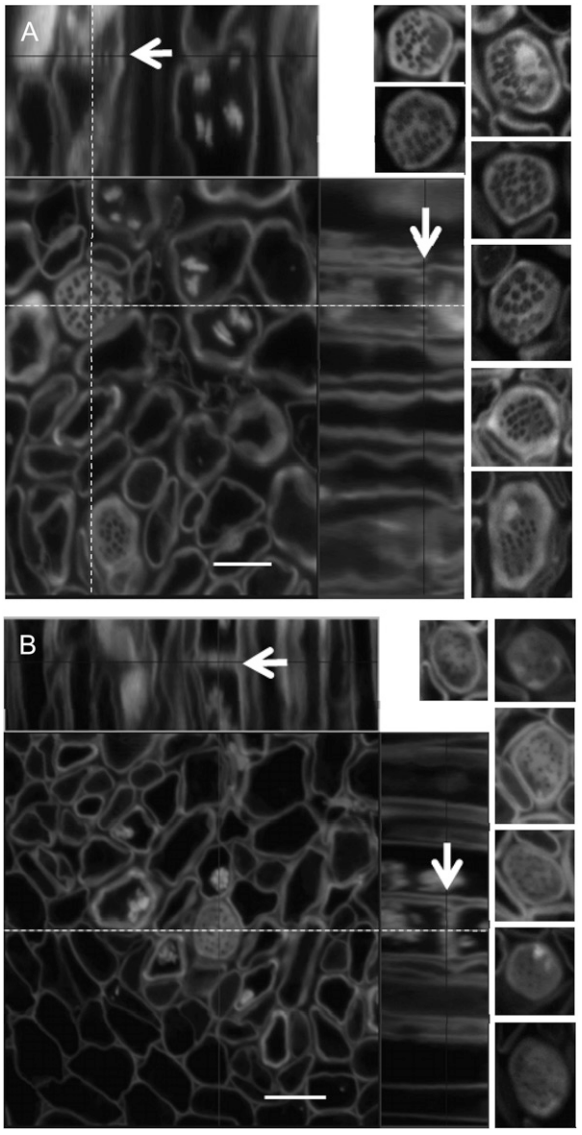

Figure 4. Sieve plate pores in the base of the stem are small or partially occluded in the *gsl7* mutant. Main images are confocal laser scanning micrographs of thick sections from the basal 4 cm of the flowering stems of 6-week-old plants. At this stage, wild-type stems were approximately 13 cm high and *gsl7* mutant stems were 10 to 11 cm high (Supplemental Fig. S3). Images were processed using Zeiss LSM Image Browser software. Sieve elements are seen in transverse section and as longitudinal projections (top and right). The dotted lines indicate the positions of the longitudinal sections with respect to the transverse sections. The arrows in the longitudinal sections are positioned at the plane of the transverse section and indicate the same sieve plate. The small images to the left of the main images are typical individual sieve plates seen in transverse sections, taken from independent preparations of stems from three different batches of plants in the wild type and two batches in the case of *gsl7* mutant plants. All images are at the same scale. A, The wild type. B, The *gsl7* mutant. Note that sieve plate pores are smaller in diameter in all mutant examples than in wild-type examples. Bars = 5 μm.

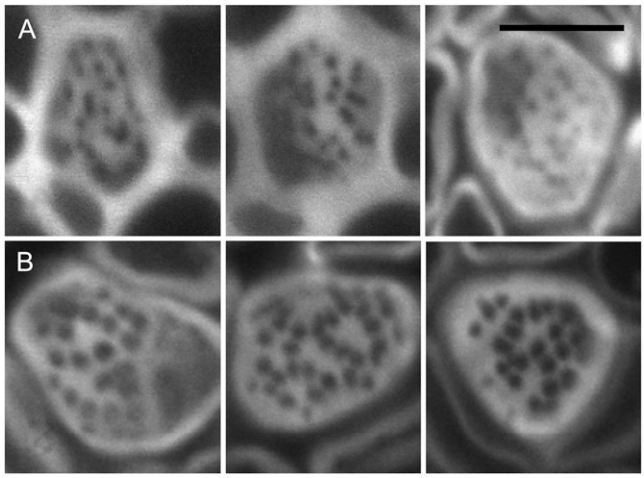

Figure 5. Phloem sieve plates in stems of *gsl7* mutant and wild-type plants. Images are taken from the batch of *gsl7* mutant plants with the largest sieve plate pores. Pore sizes were smaller in two further independently grown batches of mutant plants (Fig. 4). Images were obtained as described for Figure 4. All images are at the same magnification. A, The *gsl7* mutant. B, The wild-type, grown under the same conditions and at the same time as the *gsl7* mutant plants shown in A. Bar = 5 μm.

incorporated ^{14}C found in the stem rose to values of around 9% in both wild-type and mutant plants (Fig. 7A). However, the distribution of ^{14}C within the stem differed markedly between the genotypes. In wild-type plants, a large fraction of the ^{14}C rapidly reached the top 3 cm of the flowering stem (12–15 cm; Fig. 7B). This section contained 26% or more of the total label in the stem from 90 min onward. In *gsl7* plants, the biggest proportion of label remained in the lowest 3 cm of the stem throughout the chase (0–3 cm; Fig. 7B). This lowest section contained at least 40% of the total ^{14}C in the stem throughout the chase period. The percentage of ^{14}C in the top section rose very slowly during the chase period to a maximum value of only 3.8% of the total ^{14}C in the stem.

The difference in inflorescence architecture between wild-type and *gsl7* plants is unlikely to account for the radical differences in the rate of movement of ^{14}C in the stem. First, we compared mutant and wild-type plants with stems of the same height (rather than plants of the same age, which would have stems of different heights). Second, although *gsl7* inflorescences have different side-branch growth rates from wild-type plants, the lowest 3 cm of the stem had no or only single branches in all the plants we used. A more likely explanation of the difference in ^{14}C movement is that the rate of phloem transport in stems of *gsl7* mutants is much lower than that of wild-type plants.

Restricted phloem transport in the flowering stem of *gsl7* mutants might be expected to lead to reduced carbohydrate availability at the top of the inflorescence. Accordingly, we measured carbohydrates in the terminal cluster of flowers and buds in mutant and wild-type plants. At the end of the night, *gsl7* mutant inflorescences had half of the Suc content of wild-type inflorescences, 40% of the starch content, 30% of the Fru content, and less than 20% of the Glc content. These differences decreased through the day as contents of all carbohydrates increased (Fig. 8).

Iodine staining revealed that the difference in starch content between mutant and wild-type inflorescences was particularly marked in the parenchymatous pith at the top of the stem. At the end of the night, this tissue stained darkly in wild-type plants but not in mutant plants (Supplemental Fig. S4).

In leaves, abnormally low carbohydrate contents lead to widespread changes in gene expression. This "starvation response" is seen, for example, when the night is extended beyond the normal dawn and in mutants defective in the storage or utilization of starch reserves during the night (Smith and Stitt, 2007). The starvation response can be monitored by measuring transcript levels of genes for which expression is known to be specifically responsive to carbohydrate levels (Gibon et al., 2004; Bläsing et al., 2005; Osuna et al., 2007; Usadel et al., 2008; Graf et al., 2010). We investigated whether the reduced carbohydrate levels in the terminal cluster of flowers and buds of *gsl7* inflorescences triggered a starvation response by determining the expression of four starvation-induced genes (At1g76410, At3g59940, At1g08630, and At1g10070) and one sugar-induced gene (At3g13470; Supplemental Table S4). Transcript levels of the four starvation-induced genes were very low in both wild-type and mutant inflorescences at the end of the day. In the wild type, transcript levels remained low throughout the normal night. In the *gsl7* mutant, transcript levels of all four genes increased significantly during the night. Levels for three of the genes were significantly higher in mutant than in wild-type inflorescences at the end of the night (Fig. 9). An extension of the night by 4 h markedly increased this difference: levels were 2.7 to more than five times higher in mutant than in wild-type inflorescences. For the sugar-induced gene, transcript levels in wild-type inflorescences were more than twice as high as those in mutant inflorescences at the end of the day. This difference was maintained as transcript levels fell through the night and during the extended night (Fig. 9).

Reduced capacity for the transport of sugars to the inflorescence might be expected to lead to an accumulation of carbohydrate in leaves. Although the pattern of carbohydrate turnover in leaves of flowering Arabidopsis plants varies somewhat between batches of plants (B. Kular, M. Pike, and A.M. Smith, unpublished data), we consistently observed elevated levels of starch in leaves of the *gsl7* mutant from the onset of flowering. Leaves of 7-week-old mutant plants stained more darkly with iodine at the end of the night than leaves of wild-type plants of the same age (Supplemental Fig. S4). Mutant leaves had three times more starch than wild-type leaves at the end of the night at 5 weeks old and four times more at 6 weeks old (Fig. 8B).

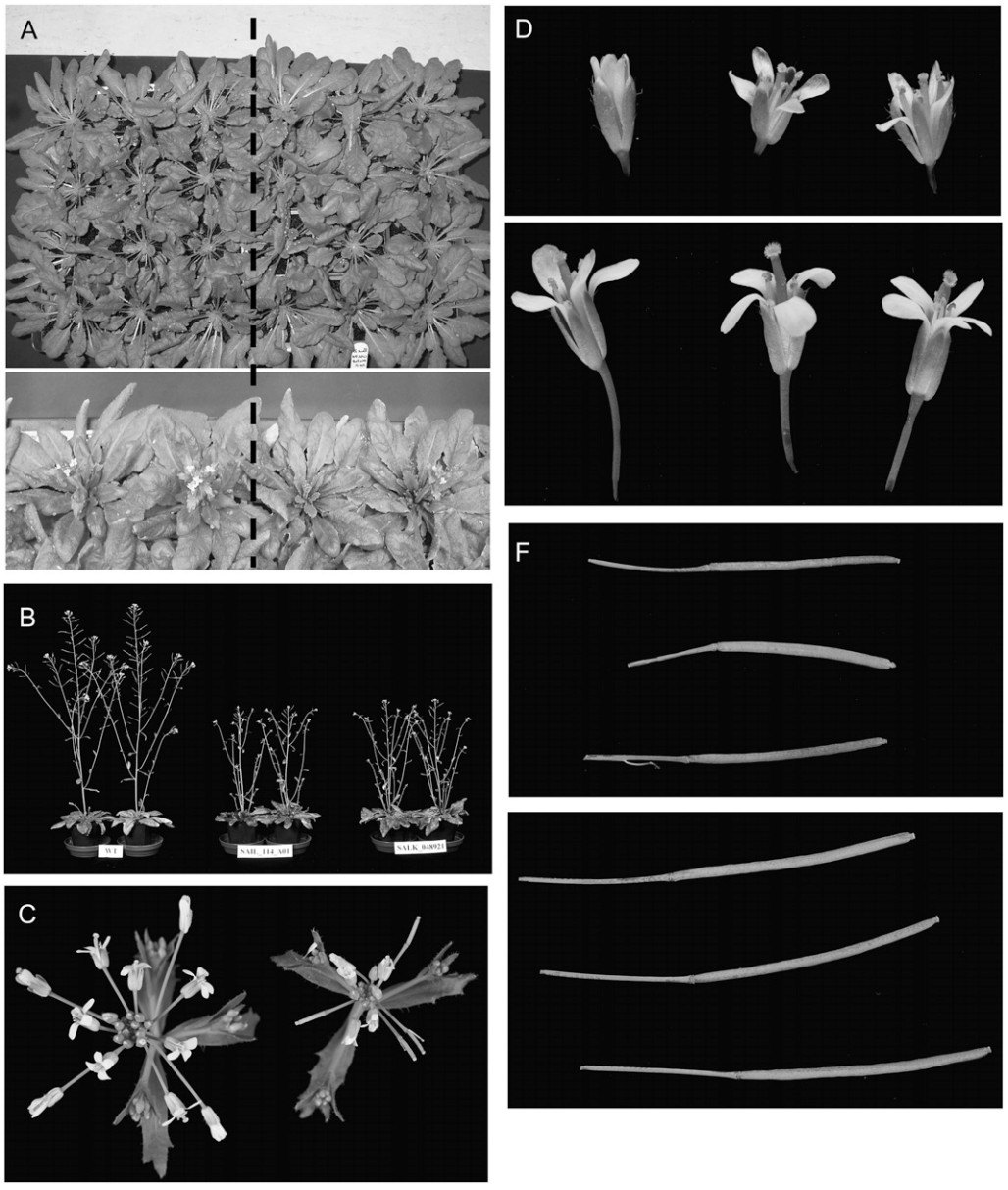

Figure 6. Vegetative and reproductive growth of the *gsl7* mutant. A, Top, plants after 45 d of growth in 8 h of light and 16 h of dark; bottom, plants after about 35 d of growth in 12 h of light and 12 h of dark. Plants to the left of the dashed line are the wild type, and those to the right are *gsl7* mutants grown in the same tray. B, Plants of the wild type (left), *gsl7-1* (middle), and *gsl7-2* (right) after 49 d of growth in 12 h of light and 12 h of dark. C, Apex of flowering stems after 42 d of growth of wild-type (left) and *gsl7* mutant (right) plants photographed from above. Photographs of plants of this age from the side are shown in Supplemental Figure S4. D, Typical flowers from the apex of the flowering stem after 42 d of growth from a *gsl7* mutant (top) and a wild-type (bottom) plant. The two images are at the same magnification. E, Fully expanded siliques from flowering stems after 42 d of growth from a *gsl7* mutant (top) and a wild-type (bottom) plant. The two images are at the same magnification.

Suc Feeding Increases Flower Size in the *gsl7* Mutant

If the reduced growth of floral parts of the *gsl7* mutant is indeed due to limited carbohydrate availability, an increased supply of Suc might be expected to increase flower size. Accordingly, we identified plants of 6 to 7 weeks old with inflorescences of the same height (total stem length of approximately 10 cm), removed the top 2 cm of the flowering stem from some of them, and placed the bases of the cut stems in a nutrient solution with or without 167 mM (3%, w/v) Suc. After 7 d of further growth under the same conditions of light, temperature, and humidity, cut inflorescences were compared with those developed for the same length of time on the intact control plants. Although the size of flowers and siliques on the cut inflorescences varied somewhat between experiments,

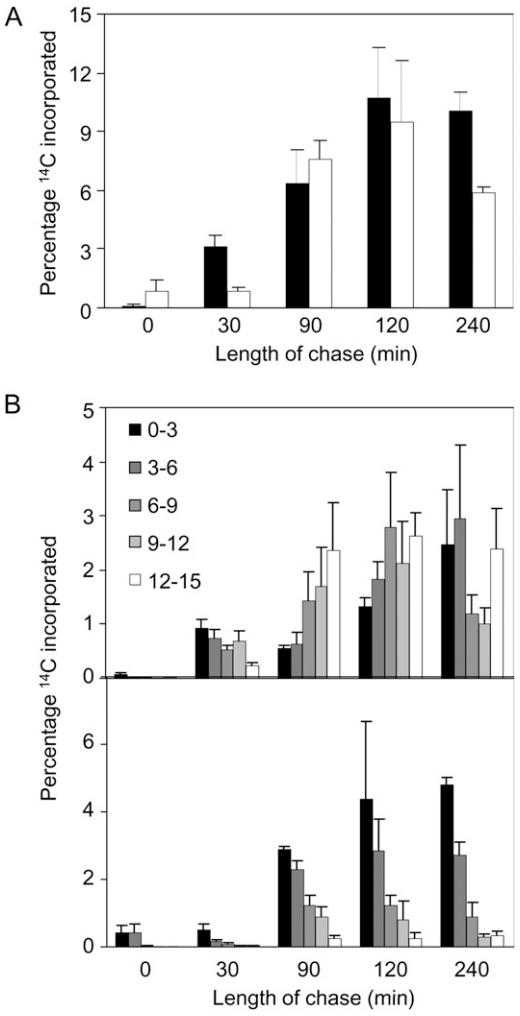

Figure 7. Rates of ^{14}C movement in the flowering stem are very different in wild-type and *gsl7* mutant plants. A 5-min pulse of $^{14}CO_2$ was supplied to a mature leaf of plants with flowering stems 15 cm high, and then plants were incubated in normal air for up to 240 min. Plants were harvested immediately after the pulse and at intervals thereafter. ^{14}C was measured in the supplied leaf and in 3-cm sections of the stem, and contents of stem sections are expressed as percentages of the total ^{14}C content (sum of supplied leaf and stem contents). Values are means of measurements on five plants for each time point, and SE is indicated. A, Percentage of ^{14}C present in the stem. Black bars, the wild-type; white bars, the *gsl7* mutant. B, Percentage of ^{14}C present in successive 3-cm sections of the stem. Section 0 to 3 is the basal section, and section 12 to 15 is the top section. Top graph, wild-type plants; bottom graph, *gsl7* mutant plants.

those incubated with Suc were in every case (three independent experiments) markedly larger than those developed on the plant (Fig. 10). This effect was entirely dependent on the presence of Suc in the nutrient solution. Almost no growth occurred in cut inflorescences in the nutrient solution without Suc (Fig. 10) or in the nutrient solution in which Suc was replaced by the same concentration of mannitol (data not shown).

DISCUSSION

GSL7 Is Responsible for Callose Deposition in Sieve Plate Pores

We provide evidence that the callose synthase GSL7 is exclusively responsible for the synthesis of callose associated with the pores of sieve plates. In the root, transcription of *GSL7* is confined to the phloem. Loss of expression of this gene results in complete loss of the callose lining of sieve plate pores between phloem sieve elements in both roots and flowering stems. Thus, it appears that none of the other 11 GSL isoforms in the plant is able to compensate for loss of GSL7 with

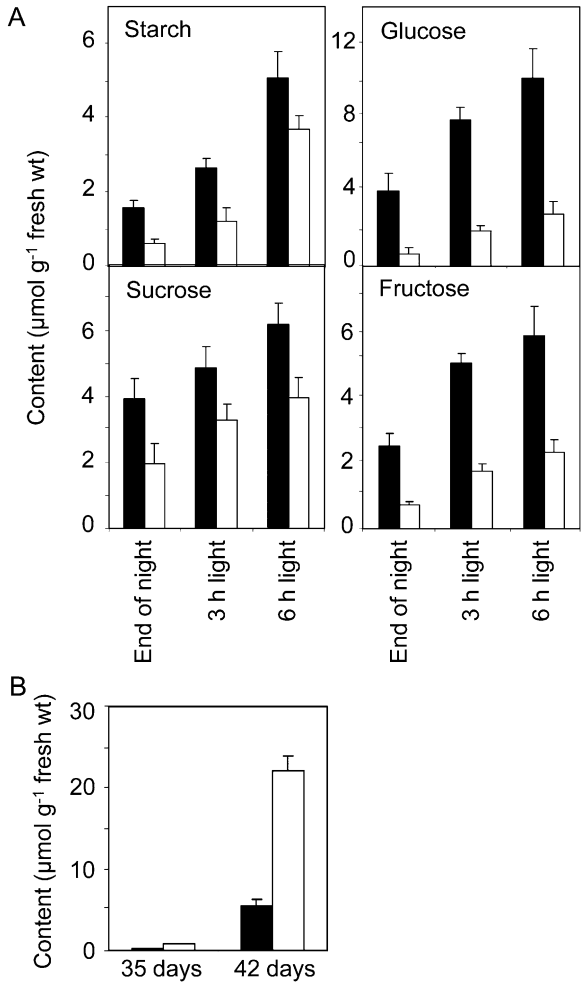

Figure 8. Carbohydrate contents of the apices of flowering stems and of leaves of mutant and wild-type plants. Values are means of measurements on five samples per time point, and SE is indicated. Black bars, the wild type; white bars, the *gsl7* mutant. A, Starch and sugars in apices of flowering stems. Plants were grown for 46 d in 12 h of light and 12 h of dark. Samples were harvested at the end of the night and 3 and 6 h into the light period. Each sample consisted of two flower heads (approximately the apical 1 cm of the main stem, consisting of the terminal cluster of flowers and buds). B, Starch in leaves. Plants were grown for either 35 or 42 d. Each sample was harvested at the end of the night and consisted of three fully expanded leaves from a single plant.

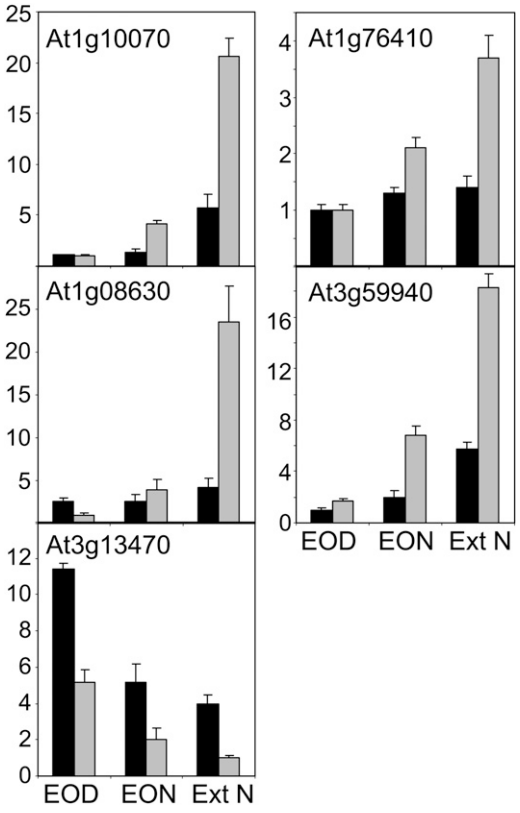

Figure 9. Expression of starvation marker genes in the apices of flowering stems of mutant and wild-type plants. Plants were grown for 42 d in 12 h of light and 12 h of dark. Samples were harvested at the end of the night (EON), end of the day (EOD), and after a 4-h extension of the night (Ext N). Each sample consisted of four flower heads (approximately the apical 1 cm of the main stem, consisting of the terminal cluster of flowers and buds). Total RNA was extracted, cDNA was synthesized, and transcript levels were measured by quantitative real-time PCR and normalized against a *UBIQUITIN10* control. Details of genes are given in Supplemental Table S4. Values are means of measurements on five samples per time point, and SD is indicated. Black bars, the wild type; gray bars, the *gsl7* mutant.

respect to the synthesis of callose in stem or root phloem. Callose in several other tissues of the plant seems to be unaffected. Plants lacking GSL7 do not display the loss of fertility seen in plants in which callose is not deposited during male gametogenesis (*gsl8* and *gsl10* mutants; Töller et al., 2008) or the extreme growth phenotypes seen when callose deposition on cell plates during cytokinesis is compromised (*gsl8* mutants; Töller et al., 2008; Chen et al., 2009). Loss of GSL7 does not affect the formation of wound callose in leaf mesophyll cells and in parts of the stem other than the phloem. Thus, the synthesis of callose via GSL7 seems to be confined to the phloem sieve elements.

Our data indicate that GSL7 is responsible for the synthesis of callose in the sieve plate pore both as part of the normal process of phloem maturation in intact plants and also in response to wounding. First, callose is present in phloem sieve plates of wild-type plants but absent from those of *gsl7* mutants when precautions are taken to avoid a wound response by fixing excised tissue as rapidly as possible. Second, the striking reduction in growth of the stem in the *gsl7* mutant is consistent with a role for GSL7 in the intact, nonwounded plant. Third, callose is not deposited in the phloem of *gsl7* mutant plants after wounding, implying that GSL7 is required for the rapid occlusion of the sieve plate by callose in response to wounding. The pattern of expression of *GSL7* is consistent with roles in both the developing and the mature phloem. We detected *GSL7* transcript in phloem initial cells in the root by in situ hybridization. GSL7 protein synthesized in these cells is likely to be responsible for callose deposition during sieve plate formation. *GSL7*

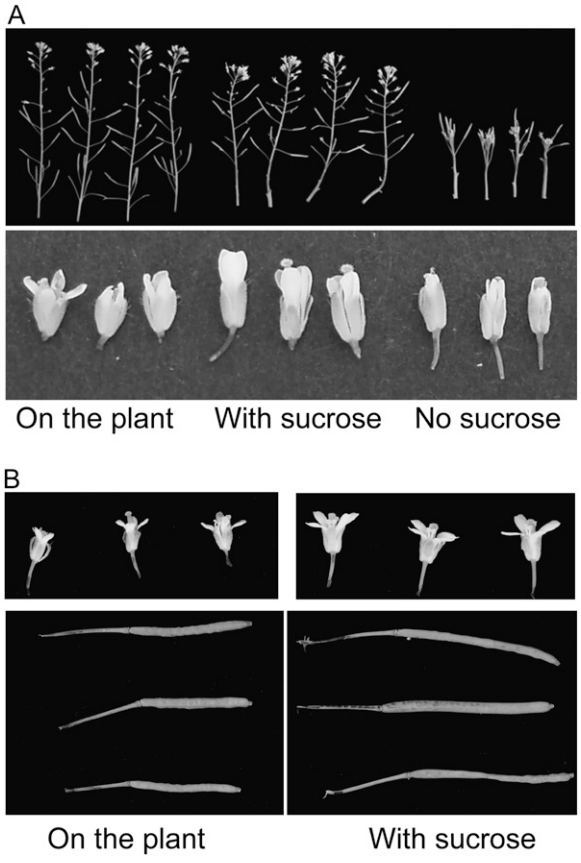

Figure 10. Effects of Suc feeding on the inflorescence of the *gsl7* mutant. The apical 2 cm of flowering stems of half of a batch of *gsl7* plants was harvested when flowering stems were approximately 10 cm in height, and the cut base was incubated in a solution with or without 167 mM Suc. Cultured stems and the remaining intact plants were held in the same environmental conditions for 7 d. A, Inflorescences (top) and flowers (bottom) of intact plants (left), stems cultured with Suc (middle), and stems cultured without Suc (right). B, Flowers (top) and siliques (bottom) from an experiment on a separately grown batch of plants. Left, Organs from intact plants; right, organs from stems cultured with Suc. The two images of flowers are the same magnification, as are the two images of siliques.

transcript is also present in the mature phloem (detected by microarray analysis of marked, sorted cell types in the root; Arex database, http://www.arexdb.org/). We suggest that GSL7 protein synthesized in the companion cells of the mature phloem is responsible for the production of callose on the sieve plates of the sieve elements in response to wounding. It is also possible that GSL7 is involved in callose turnover in mature sieve plate pores in intact plants. Turnover of callose deposits in the neck regions of plasmodesmata is proposed to alter the diameter of the plasmodesmatal pore and thus control plasmodesmatal fluxes (Levy et al., 2007). Similarly, turnover of callose in the sieve plate pore in response to developmental and/or environmental factors may alter the diameter of the pore and thus modulate phloem conductivity.

Callose Synthesis in the Phloem May Differ from That in Other Parts of the Plant

It has been suggested that UDPglucose for the synthesis of cell wall components is supplied via a specific association between SUS and cell wall biosynthetic enzymes (Amor et al., 1995; Verma and Hong, 2001; Salnikov et al., 2003; Persia et al., 2008). SUS is frequently associated with plasma membranes, consistent with the idea that it supplies UDPglucose to either cellulose synthase or callose synthase or both. However, complete loss of SUS (in a *sus1sus2sus3sus4* mutant) from all cell types except the phloem in Arabidopsis has negligible effects on growth in standard conditions (Barratt et al., 2009). This suggests that SUS is not required for either cellulose or callose synthesis in most organs of the plant. Thus, UDPglucose generated in the cytosol by an alternative route (e.g. UDPglucose pyrophosphorylase) must be sufficient.

The situation in the phloem appears to be different. We showed previously that the presence of callose in the sieve plate pores is partially dependent on two isoforms of SUS located in the phloem sieve element, SUS5 and SUS6. A mutant lacking both of these isoforms had much thinner layers of callose in the sieve plate pores of the stem than wild-type plants, although inflorescence growth was normal (Barratt et al., 2009). Thus, it seems likely that these SUS isoforms synthesize the UDPglucose substrate for GSL7 from Suc in phloem. Callose synthases are membrane-spanning proteins, taking substrate from the cytosol and generating callose outside the cell. The fact that SUS5 and SUS6 are exclusively and tightly associated with a cell wall fraction in extracts of Arabidopsis tissues (requiring high salt and detergent treatments for their release; Barratt et al., 2009) suggests that they may form part of a complex involved in callose synthesis on the sieve plate. However, it seems highly unlikely that SUS5 and SUS6 are outside the cell. Both have kinetic properties, including a neutral pH optimum, similar to other, intracellular SUS isoforms (Bieniawska et al., 2007). We suggest that GSL7, SUS5, and SUS6 may form part of a tight complex that spans the plasma membrane of the sieve element and links into the wall. In this context, it is interesting that both SUS isoforms have C-terminal extensions not found in other isoforms (Baud et al., 2004); these may be involved in complex formation.

Although the callose lining of sieve plate pores is reduced in thickness in the *sus5sus6* mutant, it is not abolished. This implies that GSL7 can obtain substrate from another source, at least in this mutant. It is possible that the SUS1 isoform fulfills this role. Unlike SUS2, SUS3, and SUS4, which are entirely soluble, a minor fraction of the SUS1 protein is consistently present in the cell wall fraction of Arabidopsis extracts (Barratt et al., 2009).

The specific requirement for SUS for normal callose synthesis via GSL7 in the sieve element may reflect the highly unusual metabolic status of the sieve element. The concentration of Suc is extremely high, and concentrations of many other primary metabolites are likely to be low in relation to other cell types. Direct utilization of Suc to provide UDPglucose for callose synthesis, via SUS, may thus be favored over the synthesis of UDPglucose via UDPglucose pryophosphorylase from Glc-1-P. A direct association of SUS with the callose synthase complex may be essential to ensure an adequate concentration of UDPglucose at the active site. The source of UDP for UDPglucose synthesis in the sieve element remains an open and interesting question.

The Callose Lining of Sieve Plate Pores Is Necessary for Normal Phloem Transport in the Stem

Our results provide direct and unambiguous evidence that the callose lining of the sieve plate pore is essential for normal phloem transport in the flowering stem. In *gsl7* mutants, the growth of the stem, flowers, and siliques is strongly reduced. Labeling experiments showed that transport of Suc in the flowering stem was very strongly reduced in the *gsl7* mutant. Although the rate of entry of ^{14}C into the stem after supply of $^{14}CO_2$ to a leaf was approximately the same in wild-type and *gsl7* mutant plants, its rate of movement to the top of stem of the same height was greatly retarded in the mutant. The most likely explanation of this difference is that loss of callose from the sieve plate pores drastically reduces phloem conductivity.

Several different features of our results suggest that restricted transport of Suc in *gsl7* phloem resulted in metabolic and transcriptional changes in the inflorescences, which in turn account for their reduced size. Starch and sugar contents were lower in *gsl7* than in wild-type inflorescences, especially at the end of the night. Photosynthesis in the inflorescence of the mutant during the light period may compensate to some extent for the reduced supply of Suc via the phloem. The reduction in carbohydrate availability in the mutant inflorescence enhanced the expression of starvation genes and repressed the expression of a sugar-activated gene. Induction of expression of the starvation genes in leaves is associated with a strong reduction or cessation

of growth in both leaves and roots (Smith and Stitt, 2007; Graf et al., 2010, and refs. therein).

Further evidence for a link between reduced growth of the inflorescence of *gsl7* plants and Suc supply is provided by experiments in which Suc was supplied directly to *gsl7* inflorescences via the cut stem. Suc supplied in this way probably moves to the flowers via the xylem rather than the phloem. The result was an increase in size of all floral parts relative to those on intact mutant plants. These data are consistent with the idea that a lack of Suc alone could account for the reduced growth. None of our experiments preclude the possibility that reduced growth of the inflorescence is at least in part due to reduced transport of a hormone or other signaling molecule necessary for normal growth. However, the simplest interpretation is that reduced growth results from low carbohydrate availability brought about by reduced phloem conductivity in the stem.

The effect of the loss of GSL7 is much more marked in the inflorescence than in the rosette. The inflorescence is a major sink for carbon from the rosette, and the marked phenotype likely reflects its dependence on, and distance from, source organs. It is interesting that there is no marked impact of the *gsl7* mutation on root mass in mature rosettes even though root sieve plate pores lack callose. This difference in impact of the mutation between stems and roots may reflect a higher demand for carbon by the developing inflorescence than by the root system. We have not examined the phloem of developing (sink) leaves and petioles. It remains possible that another enzyme in part compensates for the loss of GSL7 in these organs.

The Callose Lining May Determine the Flow Characteristics of the Sieve Plate Pore

It is not immediately apparent why loss of the callose lining of the sieve plate pore should cause a dramatic reduction in phloem transport in the stem. One possibility is that callose is required for normal sieve plate pore development. Some authors have proposed that during this process existing wall components around plasmodesmata are replaced by callose, which is then degraded to form a pore (see introduction). If this is the case, loss of callose is expected to prevent or very seriously restrict pore formation. Our data do not support this idea. It is clear that degradation of noncallose wall material in the *gsl7* mutant allows the formation of pores at approximately the same frequency as in wild-type plants. From transmission electron microscopy (TEM) images, the pores in *gsl7* plants appear to be of approximately the same dimensions as those in wild-type plants. Thus, we suggest that callose deposition is not required for pore formation per se. However, callose formation during pore development may nonetheless be important in determining the flow characteristics of the pore. Some authors have noted that deposition of callose on the face of the end wall where the pore will form is associated with the cessation of wall thickening at that point, so that in the mature sieve plate, the pore openings are in slight depressions in the face of the wall (Evert et al., 1966; Deshpande, 1974, 1975). It is proposed that callose actually restricts wall growth. The length of the pore is important in determining phloem conductivity (Thompson and Holbrook, 2003), so this proposed role for callose may be of significance in the function of the mature phloem. Our TEM images are consistent with the suggestion that callose deposition may reduce effective pore length, although further work would be required to confirm this point. Whereas pore openings in the *gsl7* mutant tend to be flush with the surface of the wall, those in wild-type plants are surrounded by callose-lined depressions (Fig. 2).

An alternative explanation for the importance of the callose in the sieve plate pore is that it provides necessary mechanical strength to the pore walls. Phloem conductivity and transport velocity are highly dependent on pore diameter (Thompson and Holbrook, 2003). In an intact plant, the pores must remain open against the mechanical stress imposed by the mass flow of viscous material in the sieve element. It seems likely that the callose lining renders the sieve plate pore a rigid, noncompressible tube with good flow characteristics. In the absence of a rigid lining, the diameter of the pore may vary with flow velocity, the walls tending to deform under pressure. There may also be variation within the cross-section of the wall in the tendency to deform under pressure, to the further detriment of the flow characteristics. Although the mechanical properties of callose are not well understood, it is clear that it provides resistance to both tension and compression stress in the walls of pollen tubes. Enzymatic removal of callose from pollen tubes halved the stiffness (N m^{-1}) of the side wall of the tube (Parre and Geitmann, 2005). We suggest that in the *gsl7* mutant, the walls of the sieve plate pore tend to collapse under mass flow, reducing phloem conductivity and hence the supply of Suc to the inflorescence. It is not yet clear why our confocal laser scanning microscopy views of sieve plates showed a large reduction in the apparent diameter of sieve plate pores in mutant stems relative to wild-type stems when this was not seen in TEM images. This difference could reflect plasticity of the wall of the pore of the mutant. In the absence of a rigid callose lining, the pore walls may swell or shrink differentially in the two different fixation and preparation techniques used for TEM and confocal laser scanning microscopy.

In summary, we suggest that callose deposition is not required for pore formation per se but is a very important determinant of the flow characteristics of the pore. Callose may influence both the effective length of the pore, by preventing wall thickening around the developing pore, and its flow characteristics, by providing a rigid lining and hence an invariant diameter under mass flow conditions.

After acceptance of this paper, we became aware of another paper published online that also reports the

importance of GSL7 for callose synthesis in the phloem (Xie et al., 2010). The authors propose that the loss of callose in *gsl7* mutants hampers sieve plate pore formation, whereas our work indicates that pore function rather than pore formation is hampered. Further research will be required to resolve this issue.

MATERIALS AND METHODS

Plant Material

Unless otherwise stated, Arabidopsis (*Arabidopsis thaliana*) plants were grown in compost at 20°C with a 12-h-light/12-h-dark cycle, 150 to 200 μmol quanta photosynthetically active radiation m^{-2} s^{-1}, and 75% relative humidity. For seedlings and seedling roots, seeds were surface sterilized, sown on plates of solid medium, and grown vertically at 22°C with 6 h of dark and 18 h of light according to Barratt et al. (2009). Homozygous mutants were identified by screening T-DNA insertion lines from the SALK collection and SAIL lines with gene- and T-DNA-specific primers. Studies were carried out on the *gsl7-1* mutant unless otherwise stated. Primer sequences are given in Supplemental Table S5. Genomic DNA was extracted from leaves according to Krysan et al. (1996). The PCR products obtained using T-DNA left border primers and gene-specific primers were sequenced to confirm the locations of the inserts. A wild-type line was selected as a control for each mutant line from the segregating F2 population from which the mutant was selected.

Inflorescence Culture

Flowering stems of 6- to 7-week-old plants were cut 2 cm below the apex and then immediately recut under sterile water. Cut ends were sterilized in 0.025% (v/v) sodium hypochlorite for 5 min. The cut ends were then inserted through holes in the lid of a petri dish containing filter-sterilized medium (one-quarter-strength Arabidopsis nutrient solution [Arteca and Arteca, 2000]) with 3% (w/v) Suc, 20 mM L-Gln, and 10 mM L-Asn to a depth of about 0.75 cm. The stems were cultured for 7 d, and the medium was changed daily. Culture was in the same controlled-environment conditions used for the growth of intact plants.

In Situ Hybridization

Primer sequences are given in Supplemental Table S5. A DNA template for a partial cDNA for *GSL7* was generated from a stem cDNA library by PCR, and T3 (sense) and T7 (antisense) promoter sequences were incorporated by PCR to give 350-bp probes. Whole-mount in situ hybridization on 4-d-old seedlings using digoxigenin-labeled probes was carried out according to Carol et al. (2005) and Barratt et al. (2009).

Microscopy

For confocal laser scanning microscopy on thick sections, the basal 4 cm of primary flowering stems of 6-week-old plants was excised and immediately fixed in ice-cold 50% (v/v) methanol and 10% (v/v) acetic acid for at least 24 h. The stem was recut, and sections of the basal 2 cm were sectioned under absolute ethanol on a Vibratome. Sections (200 μm) were transferred to fixative and then subjected to pseudo-Schiff propidium iodide staining (Truernit et al., 2008). Samples were viewed with a confocal microscope at an excitation wavelength of 488 nm.

TEM and immunogold labeling of phloem in longitudinal sections of the basal 4 cm of primary flowering stems of 6-week-old plants and of the basal 2 cm of the main root of 11-d-old seedlings, grown on solid medium, were carried out as described by Barratt et al. (2009). To ensure rapid cessation of metabolism, excised tissue was immediately placed into fixative (2.5% [v/v] glutaraldehyde in 0.05 M sodium cacodylate, pH 7.3), rapidly sliced into 1-mm pieces, and then vacuum infiltrated with fixative.

Aniline Blue and Iodine Staining

Hand-cut sections of primary flowering stems from 6- to 7-week-old plants were stained with 0.1% (w/v) aniline blue (water soluble; Sigma) in 0.1 M sodium phosphate (pH 9.0) and then viewed with a UV epifluorescence microscope.

For leaf wounding, fully expanded leaves from 6-week-old plants were punctured with a plastic tip and then harvested the next day. After removal of chlorophyll by washing in methanol, leaves were rinsed in water and stained overnight with aniline blue as above.

For roots, whole 4-d-old seedlings were vacuum infiltrated with 0.1% (w/v) aniline blue in 0.1 M sodium phosphate (pH 9.0) and incubated in the dark for 1 to 2 h.

Starch in the apical region of primary flowering stems was visualized by staining with Lugol's iodine solution after removal of chlorophyll at 80°C in 80% (v/v) ethanol.

Metabolite Assays

For starch and sugar measurements, tissue was frozen in liquid nitrogen immediately after harvest. Tissue was extracted with dilute perchloric acid. Sugars were assayed enzymatically on the neutralized soluble fraction using spectrophotometric assays coupled to NAD reduction via Glc-6-P dehydrogenase (Chia et al., 2004). Starch was assayed as Glc in the insoluble fraction after washing, gelatinization, and enzymatic digestion with α-amylase and α-amyloglucosidase (Smith and Zeeman, 2006).

Quantitative Real-Time PCR Analysis

Each sample consisted of the terminal cluster of flowers and buds from the primary flowering stems of four 6-week-old plants. Total RNA was isolated using the RNeasy kit (Qiagen) and digested with RQ1 RNase-Free DNase 1 (Promega). cDNA was synthesized using the SuperScript 111 kit (Invitrogen). Quantitative real-time PCR was performed on a 96-well plate with a DNA Engine Opticon 2 Real-Time PCR Detection System (Bio-Rad) in a reaction mix containing 5 μL of SYBR Green JumpStart Taq ReadyMix (Sigma). Thermal cycling was 95°C for 2 min and 40 cycles of 95°C for 10 s, 60°C for 1 min. Primer sequences are given in Supplemental Table S5. Values were normalized against a *UBIQUITIN10* control, and relative expression was calculated by setting the wild-type value to 1.

$^{14}CO_2$ Pulse-Chase Labeling

Labeling experiments were performed 2 h into the photoperiod on intact flowering plants in principal growth stage 6 (Boyes et al., 2001) with a primary flowering stem height of 15 cm. In a sealed reservoir chamber, $^{14}CO_2$ with a specific activity of 59 mCi $mmol^{-1}$ was released by the acidification of sodium ^{14}C-bicarbonate. A small plexiglass chamber connected to the reservoir was clamped to a mature adult leaf of a plant illuminated with 150 μmol quanta photosynthetically active radiation m^{-2} s^{-1}. $^{14}CO_2$ was circulated for 5 min, after which the plexiglass chamber was removed and the plants were kept in normal air for a chase period of 0 to 240 min.

Three-centimeter sections of the flowering stem and the labeled leaf were harvested separately into tubes containing 5 mL of 80% (v/v) boiling ethanol. Samples were homogenized using a glass homogenizer and successively extracted for 5 min in 3 mL of 80% (v/v) ethanol, 50% (v/v) ethanol, 20% (v/v) ethanol, water, and finally 80% (v/v) ethanol. Between each extraction, insoluble material was removed by centrifugation. For each sample, the combined supernatants were dried down under an air stream. This fraction was redissolved in 2 mL of water. Any water-insoluble residue was dissolved in 1 mL of 98% (v/v) ethanol. The insoluble material was resuspended in tissue solubilizer (NCS; GE Healthcare) and dissolved overnight at 23°C. Liquid scintillation counting was used to determine the ^{14}C in each fraction.

Supplemental Data

The following materials are available in the online version of this article.

Supplemental Figure S1. Location in roots of transcripts for *SUS5*, *SUS6*, and *GSL7*.

Supplemental Figure S2. Absence of *GSL7* transcript in two lines carrying T-DNA insertions in the *GSL7* gene.

Supplemental Figure S3. Growth of wild-type and *gsl7* mutant plants.

Supplemental Figure S4. Loss of starch from the inflorescence and altered starch turnover in the leaves of the *gsl7* mutant.

Supplemental Table S1. Top 20 genes coexpressed with *SUS5* (At5g37180), from ATTED-II.

Supplemental Table S2. Top 40 genes coexpressed with *SUS5* (At5g37180), from CSB.DB.

Supplemental Table S3. Weights of rosettes, leaves, and stem bases of wild-type and mutant plants.

Supplemental Table S4. Starvation marker genes used in this study.

Supplemental Table S5. Primers used in this study.

ACKNOWLEDGMENTS

We thank Susan Bunnewell and Paul Derbyshire (both John Innes Centre) for help with TEM and advice on in situ hybridization, respectively.

Received September 20, 2010; accepted November 18, 2010; published November 22, 2010.

LITERATURE CITED

Amor Y, Haigler CH, Johnson S, Wainscott M, Delmer DP (1995) A membrane-associated form of sucrose synthase and its potential role in synthesis of cellulose and callose in plants. Proc Natl Acad Sci USA **92:** 9353–9357

Arteca RN, Arteca JM (2000) A novel method for growing *Arabidopsis thaliana* plants hydroponically. Physiol Plant **108:** 188–193

Barratt DHP, Derbyshire P, Findlay K, Pike M, Wellner N, Lunn J, Feil R, Simpson C, Maule AJ, Smith AM (2009) Normal growth of *Arabidopsis* requires cytosolic invertase but not sucrose synthase. Proc Natl Acad Sci USA **106:** 13124–13129

Baud S, Vaultier MN, Rochat C (2004) Structure and expression profile of the sucrose synthase multigene family in *Arabidopsis*. J Exp Bot **55:** 397–409

Bieniawska Z, Barratt DHP, Garlick AP, Thole V, Kruger NJ, Martin C, Zrenner R, Smith AM (2007) Analysis of the sucrose synthase gene family in Arabidopsis. Plant J **49:** 810–828

Birnbaum K, Shasha DE, Wang JY, Jung JW, Lambert GM, Galbraith DW, Benfey PN (2003) A gene expression map of the *Arabidopsis* root. Science **302:** 1956–1960

Bläsing OE, Gibon Y, Günther M, Höhne M, Morcuende R, Osuna D, Thimm O, Usadel B, Scheible WR, Stitt M (2005) Sugars and circadian regulation make major contributions to the global regulation of diurnal gene expression in *Arabidopsis*. Plant Cell **17:** 3257–3281

Bouck GB, Cronshaw J (1965) The fine structure of differentiating sieve tube elements. J Cell Biol **25:** 79–95

Boyes DC, Zayed AM, Ascenzi R, McCaskill AJ, Hoffman NE, Davis KR, Görlach J (2001) Growth stage-based phenotypic analysis of *Arabidopsis*: a model for high throughput functional genomics in plants. Plant Cell **13:** 1499–1510

Brady SM, Orlando DA, Lee JY, Wang JY, Koch J, Dinneny JR, Mace D, Ohler U, Benfey PN (2007) A high-resolution root spatiotemporal map reveals dominant expression patterns. Science **318:** 801–806

Carol RJ, Takeda S, Linstead P, Durrant MC, Kakesova H, Derbyshire P, Drea S, Zarsky V, Dolan L (2005) A RhoGDP dissociation inhibitor spatially regulates growth in root hair cells. Nature **438:** 1013–1016

Cartwright DA, Brady SM, Orlando DA, Sturmfels B, Benfey PN (2009) Reconstructing spatiotemporal gene expression data from partial observations. Bioinformatics **25:** 2581–2587

Chen XY, Liu L, Lee E, Han X, Rim Y, Chu H, Kim SW, Sack F, Kim JY (2009) The Arabidopsis callose synthase gene *GSL8* is required for cytokinesis and cell patterning. Plant Physiol **150:** 105–113

Chia T, Thorneycroft D, Chapple A, Messerli G, Chen J, Zeeman SC, Smith SM, Smith AM (2004) A cytosolic glucosyltransferase is required for conversion of starch to sucrose in *Arabidopsis* leaves at night. Plant J **37:** 853–863

Deshpande BP (1974) Development of the sieve plate in *Saxifraga sarmentosa* L. Ann Bot (Lond) **38:** 151–158

Deshpande BP (1975) Differentiation of the sieve plate of *Cucurbita*: a further view. Ann Bot (Lond) **39:** 1015–1022

Dong X, Hong Z, Chatterjee J, Kim S, Verma DPS (2008) Expression of callose synthase genes and its connection with Npr1 signaling pathway during pathogen infection. Planta **229:** 87–98

Ehlers K, Knoblauch M, van Bel AJE (2000) Ultrastructural features of well-preserved and injured sieve elements: minute clamps keep the phloem transport conduits free for mass flow. Protoplasma **214:** 80–92

Eleftheriou EP (1990) Microtubules and sieve plate development in differentiating protophloem sieve elements of *Triticum aestivum* L. J Exp Bot **41:** 1507–1515

Enns LC, Kanaoka MM, Torii KU, Comai L, Okada K, Cleland RE (2005) Two callose synthases, GSL1 and GSL5, play an essential and redundant role in plant and pollen development and in fertility. Plant Mol Biol **58:** 333–349

Esau K, Thorsch J (1985) Sieve plate pores and plasmodesmata, the communication channels of the symplast: ultrastructural aspects and developmental relations. Am J Bot **72:** 1641–1653

Evert RF, Derr WF (1964) Callose substance in sieve elements. Am J Bot **51:** 552–559

Evert RF, Murmanis L, Sachs IB (1966) Another view of the ultrastructure of *Cucurbita* phloem. Ann Bot (Lond) **30:** 563–585

Gibon Y, Bläsing OE, Palacios-Rojas N, Pankovic D, Hendriks JHM, Fisahn J, Höhne M, Günther M, Stitt M (2004) Adjustment of diurnal starch turnover to short days: depletion of sugar during the night leads to a temporary inhibition of carbohydrate utilization, accumulation of sugars and post-translational activation of ADP-glucose pyrophosphorylase in the following light period. Plant J **39:** 847–862

Graf A, Schlereth A, Stitt M, Smith AM (2010) Circadian control of carbohydrate availability for growth in *Arabidopsis* plants at night. Proc Natl Acad Sci USA **107:** 9458–9463

Hao P, Liu C, Wang Y, Chen R, Tang M, Du B, Zhu L, He G (2008) Herbivore-induced callose deposition on the sieve plates of rice: an important mechanism for host resistance. Plant Physiol **146:** 1810–1820

Hong Z, Zhang Z, Olson JM, Verma DPS (2001) A novel UDP-glucose transferase is part of the callose synthase complex and interacts with phragmoplastin at the forming cell plate. Plant Cell **13:** 769–779

Huang L, Chen XY, Rim Y, Han X, Cho WK, Kim SW, Kim JY (2009) Arabidopsis glucan synthase-like 10 functions in male gametogenesis. J Plant Physiol **166:** 344–352

Jacobs AK, Lipka V, Burton RA, Panstruga R, Strizhov N, Schulze-Lefert P, Fincher GB (2003) An *Arabidopsis* callose synthase, GSL5, is required for wound and papillary callose formation. Plant Cell **15:** 2503–2513

Kempema LA, Cui X, Holzer FM, Walling LL (2007) Arabidopsis transcriptome changes in response to phloem-feeding silverleaf whitefly nymphs: similarities and distinctions in responses to aphids. Plant Physiol **143:** 849–865

Krysan PJ, Young JC, Tax F, Sussman MR (1996) Identification of transferred DNA insertions within Arabidopsis genes involved in signal transduction and ion transport. Proc Natl Acad Sci USA **93:** 8145–8150

Kuśnierczyk A, Winge P, Jørstad TS, Troczyńska J, Rossiter JT, Bones AM (2008) Towards global understanding of plant defence against aphids: timing and dynamics of early Arabidopsis defence responses to cabbage aphid (*Brevicoryne brassicae*) attack. Plant Cell Environ **31:** 1097–1115

Levy A, Erlanger M, Rosenthal M, Epel BL (2007) A plasmodesmata-associated β-1,3-glucanase in Arabidopsis. Plant J **49:** 669–682

McCormick S (1993) Male gametophyte development. Plant Cell **5:** 1265–1275

Mullendore DL, Windt CW, Van As H, Knoblauch M (2010) Sieve tube geometry in relation to phloem flow. Plant Cell **22:** 579–593

Nishikawa S, Zinkl GM, Swanson RJ, Maruyama D, Preuss D (2005) Callose (β-1,3 glucan) is essential for Arabidopsis pollen wall patterning, but not tube growth. BMC Plant Biol **5:** 22

Nishimura MT, Stein M, Hou BH, Vogel JP, Edwards H, Somerville SC (2003) Loss of a callose synthase results in salicylic acid-dependent disease resistance. Science **301:** 969–972

Obayashi T, Kinoshita K, Nakai K, Shibaoka M, Hayashi S, Saeki M, Shibata D, Saito K, Ohta H (2007) ATTED-II: a database of co-expressed genes and *cis* elements for identifying co-regulated gene groups in Arabidopsis. Nucleic Acids Res **35:** D863–D869

Osuna D, Usadel B, Morcuende R, Gibon Y, Bläsing OE, Höhne M, Günter M, Kamlage B, Trethewey R, Scheible WR, et al (2007) Temporal responses of transcripts, enzyme activities and metabolites after adding sucrose to carbon-deprived *Arabidopsis* seedlings. Plant J **49:** 463–491

Parre E, Geitmann A (2005) More than a leak sealant: the mechanical properties of callose in pollen tubes. Plant Physiol **137:** 274–286

Persia D, Cai G, Del Casino C, Faleri C, Willemse MTM, Cresti M (2008) Sucrose synthase is associated with the cell wall of tobacco pollen tubes. Plant Physiol **147:** 1603–1618

Rae AL, Harris PJ, Bacic A, Clarke AE (1985) Composition of the cell walls of *Nicotiana alata* Link et Otto pollen tubes. Planta **166:** 128–133

Salnikov VV, Grimson MJ, Seagull RW, Haigler CH (2003) Localization of sucrose synthase and callose in freeze-substituted secondary-wall-stage cotton fibers. Protoplasma **221:** 175–184

Samuels AL, Giddings TH Jr, Staehelin LA (1995) Cytokinesis in tobacco BY-2 and root tip cells: a new model of cell plate formation in higher plants. J Cell Biol **130:** 1345–1357

Schober MS, Burton RA, Shirley NJ, Jacobs AK, Fincher GB (2009) Analysis of the (1,3)-β-D-glucan synthase gene family of barley. Phytochemistry **70:** 713–720

Schuette S, Wood AJ, Geisler M, Geisler-Lee J, Ligrone R, Renzaglia KS (2009) Novel localization of callose in the spores of *Physcomitrella patens* and phylogenomics of the callose synthase gene family. Ann Bot (Lond) **103:** 749–756

Sjölund RD (1997) The phloem sieve element: a river runs through it. Plant Cell **9:** 1137–1146

Smith AM, Stitt M (2007) Coordination of carbon supply and plant growth. Plant Cell Environ **30:** 1126–1149

Smith AM, Zeeman SC (2006) Quantification of starch in plant tissues. Nat Protoc **1:** 1342–1345

Spanner DC (1978) Sieve-plate pores, open or occluded? A critical review. Plant Cell Environ **1:** 7–20

Thiele K, Wanner G, Kindzierski V, Jürgens G, Mayer U, Pachl F, Assaad FF (2009) The timely deposition of callose is essential for cytokinesis in Arabidopsis. Plant J **58:** 13–26

Thompson MV (2006) Phloem: the long and the short of it. Trends Plant Sci **11:** 26–32

Thompson MV, Holbrook NM (2003) Application of a single-solute non-steady-state phloem model to the study of long-distance assimilate transport. J Theor Biol **220:** 419–455

Thompson MV, Wolniak SM (2008) A plasma membrane-anchored fluorescent protein fusion illuminates sieve element plasma membranes in Arabidopsis and tobacco. Plant Physiol **146:** 1599–1610

Thorsch J, Esau K (1988) Ultrastructural aspects of primary phloem: sieve elements in poinsettia (*Euphorbia pulcherrima*, Euphorbiaceae). IAWA Bull **9:** 363–373

Töller A, Brownfield L, Neu C, Twell D, Schulze-Lefert P (2008) Dual function of Arabidopsis glucan synthase-like genes *GSL8* and *GSL10* in male gametophyte development and plant growth. Plant J **54:** 911–923

Truernit E, Bauby H, Dubreucq B, Grandjean O, Runions J, Barthélémy J, Palauqui JC (2008) High-resolution whole-mount imaging of three-dimensional tissue organization and gene expression enables the study of phloem development and structure in *Arabidopsis*. Plant Cell **20:** 1494–1503

Turgeon R, Wolf S (2009) Phloem transport: cellular pathways and molecular trafficking. Annu Rev Plant Biol **60:** 207–221

Turner A, Wells B, Roberts K (1994) Plasmodesmata of maize root tips: structure and composition. J Cell Sci **107:** 3351–3361

Usadel B, Bläsing OE, Gibon Y, Retzlaff K, Höhne M, Günther M, Stitt M (2008) Global transcript levels respond to small changes of the carbon status during progressive exhaustion of carbohydrates in Arabidopsis rosettes. Plant Physiol **146:** 1834–1861

Van As H (2007) Intact plant MRI for the study of cell water relations, membrane permeability, cell-to-cell and long distance water transport. J Exp Bot **58:** 743–756

van Bel AJE (2003) The phloem, a miracle of ingenuity. Plant Cell Environ **26:** 125–149

van Bel AJE, Ehlers K, Knoblauch M (2002) Sieve elements caught in the act. Trends Plant Sci **7:** 126–132

Verma DPS, Hong Z (2001) Plant callose synthase complexes. Plant Mol Biol **47:** 693–701

Voigt CA, Schäfer W, Salomon S (2006) A comprehensive view on organ-specific callose synthesis in wheat (*Triticum aestivum* L.): glucan synthase-like gene expression, callose synthase activity, callose quantification and deposition. Plant Physiol Biochem **44:** 242–247

Walsh MA, Melaragno JE (1976) Ultrastructural features of developing sieve elements in *Lemna minor* L.: sieve plate and lateral sieve areas. Am J Bot **63:** 1174–1183

Xie B, Wang X, Zhu M, Zhang Z, Hong Z (November 9, 2010) *CalS7* encodes a callose synthase responsible for callose deposition in the phloem. Plant J http://dx.doi.org/10.1111/j.1365-313X.2010.04399.x